



Tracking resting state connectivity dynamics in veterans with PTSD

Han Yuan^{a,b,c}, Raquel Phillips^c, Chung Ki Wong^c, Vadim Zotev^c, Masaya Misaki^c, Brent Wurfel^{c,d}, Frank Krueger^{c,e}, Matthew Feldner^f, Jerzy Bodurka^{a,b,c,*}

^a Stephenson School of Biomedical Engineering, University of Oklahoma, Norman, OK, USA

^b University of Oklahoma Institute for Biomedical Engineering, Science and Technology, Norman, OK, USA

^c Laureate Institute for Brain Research, Tulsa, OK, USA

^d Laureate Psychiatric Clinic and Hospital, Tulsa, OK, USA

^e School of Systems Biology, George Mason University, Fairfax, VA, USA

^f Department of Psychological Science, University of Arkansas, Fayetteville, AR, USA



ARTICLE INFO

Keywords:

Posttraumatic stress disorder
 Combat veterans
 Simultaneous EEG and fMRI
 Resting state networks
 Functional connectivity
 Temporal independent EEG microstates

ABSTRACT

Posttraumatic stress disorder (PTSD) is a trauma- and stressor-related disorder that may emerge following a traumatic event. Neuroimaging studies have shown evidence of functional abnormality in many brain regions and systems affected by PTSD. Exaggerated threat detection associated with abnormalities in the salience network, as well as abnormalities in executive functions involved in emotions regulations, self-referencing and context evaluation processing are broadly reported in PTSD. Here we aimed to investigate the behavior and dynamic properties of fMRI resting state networks in combat-related PTSD, using a novel, multimodal imaging approach. Simultaneous electroencephalography (EEG) and functional magnetic resonance imaging (fMRI) was employed to measure neurobiological brain activity among 36 veterans with combat-related PTSD and 20 combat-exposed veterans without PTSD. Based on the recently established method of measuring temporal-independent EEG microstates, we developed a novel strategy to integrate EEG and fMRI by quantifying the fast temporal dynamics associated with the resting state networks. We found distinctive occurrence rates of microstates associated with the dorsal default mode network and salience networks in the PTSD group as compared with control. Furthermore, the occurrence rate of the microstate for the dorsal default mode network was positively correlated with PTSD severity, whereas the occurrence rate of the microstate for the anterior salience network was negatively correlated with hedonic tone reported by participants with PTSD. Our findings reveal a novel aspect of abnormal network dynamics in combat-related PTSD and contribute to a better understanding of the pathophysiology of the disorder. Simultaneous EEG and fMRI will be a valuable tool in continuing to study the neurobiology underlying PTSD.

1. Introduction

Posttraumatic stress disorder (PTSD) is a psychiatric disorder that may emerge following a traumatic event (American Psychiatric Association [APA], 2013). It is a chronic and debilitating psychiatric disorder with characteristic symptoms of hypervigilance and hyperarousal, emotional numbing, dissociation, negative alterations in cognitions, and re-experiencing phenomena (APA, 2013; Kessler, 2000). PTSD is common following combat experiences at military deployments, particularly those in Iraq and Afghanistan (Hoge et al., 2004). The neuropathophysiology of PTSD have become investigated in neuroimaging studies. Functional magnetic resonance imaging (fMRI) studies have reported functional abnormalities in cortical and subcortical circuits involving the amygdala, insula, ventromedial

prefrontal cortex (vmPFC), posterior cingulate cortex (PCC), anterior cingulate cortex (ACC) and hippocampus (Pitman et al., 2012; Shin and Liberzon, 2010). Activation patterns of these discrete anatomical entities in response to emotion elicitation, such as the presentation of traumatic event cues, have been the focus of examination. However, it is not clear whether the abnormal patterns observed in the neural circuits are specific to reactivity to experimental emotion elicitation or if they reflect more general functional abnormalities. Therefore, identifying dysregulated patterns of resting state functional connectivity (Fox and Raichle, 2007; Greicius et al., 2009), which is examined in the absence of external tasks, may provide valuable insights into the pathophysiology of PTSD.

Resting state functional connectivity (RSFC) refers to correlations in hemodynamic activity levels among different brain regions, suggesting

* Corresponding author at: Laureate Institute for Brain Research, 6655 S. Yale Avenue, Tulsa, OK 74136-3326, USA.
 E-mail address: jbodurka@laureateinstitute.org (J. Bodurka).

synchronization of neural activation of those regions during rest (Greicius et al., 2009). The organization of the connectivity is structured as a set of resting state networks (RSNs; Biswal et al., 1995; Fox and Raichle, 2007), and regions within a RSN shows spontaneous and coherent activities. The alterations in two specific networks may underlie PTSD: the default mode network (DMN; Bluhm et al., 2009; Daniels et al., 2011; Lanius et al., 2010; Lui et al., 2009; Shin et al., 2009; Sripada et al., 2012a), and the salience network (SN; Daniels et al., 2010; Sripada et al., 2012b; Brown et al., 2014). To date, many studies examining integrity of network connectivity in PTSD have investigated the effect of combat exposure. However, the findings have been elusive. Conflicting results of these studies have largely depended on the selection of a control group. Alterations in resting state networks, or connectivity, have been reported in PTSD compared to civilian controls without trauma exposure (DiGangi et al., 2016; Misaki et al., 2017), trauma-exposed controls (Rabinak et al., 2011; Sripada et al., 2012b; Kennis et al., 2015a,b; Misaki et al., 2017; Miller et al., 2017), or a combination of trauma-exposed and non-trauma-exposed controls (Sripada et al., 2012a; Koch et al., 2016; Kennis et al., 2015a). Sampling both combat-exposed and civilian controls obfuscates understanding if PTSD-related differences are specific to PTSD or due to combat exposure or even being in the military more generally. In this regard, a study by DiGangi et al. (2016) examined details in three groups, i.e. veterans with combat-related PTSD, combat-exposed controls without PTSD and never-traumatized healthy controls, and compared their resting state functional connectivity. Differences associated with PTSD were only observed in comparison with the civilian control, but not in comparison with combat-exposed veterans. Thus, it remains unclear whether abnormality of resting state networks is best attributed to military status, combat exposure, or PTSD.

The goal of the current study was to test whether RSFC differs between combat-exposed veterans with, as compared to without, PTSD. This method allows for ruling out the effects of being in the military generally, and combat exposure specifically. We employed a novel multimodal imaging approach using simultaneous electroencephalography (EEG) and fMRI to study activity in the resting state networks. The measurement of neural activity via fMRI, as done in prior work, is relatively limited in terms of understanding temporal dynamics of neural activity because the BOLD signal relies on a relatively slow hemodynamic response. In contrast, EEG is much more sensitive to the temporal dynamics of neural activity because it captures fast neuronal events that evolve on the scale of milliseconds. Neuroimaging with integrated and combined EEG-fMRI has been suggested to offer new insights in the study of functional connectivity because it offers both high spatial resolution of fMRI and the high temporal resolution of EEG (He et al., 2008). In order to examine resting state network activity, a new method by Yuan et al. (2012) has demonstrated that temporal independent EEG microstates (EEG-ms) can be obtained from resting state EEG acquired concurrently with fMRI. It was further showed that EEG-ms form direct electrophysiological signatures to the canonical resting state networks measured by resting state fMRI in both spatial and temporal domains (Yuan et al., 2012, 2016). This study examined EEG-ms associated with the resting state networks of relevance to PTSD — default mode network and the salience network. We proposed a new strategy to quantify the fast temporal dynamics of DMN, and SN functional connectivity in terms of EEG-ms occurrence rate. We hypothesized to observe abnormalities in the electrophysiological signatures of the two resting state networks, default-mode network and salience network, between the PTSD group and the combat control group.

2. Methods

2.1. Participants

The study was approved by the Western Institutional Review Board (IRB). All study procedures were carried out in accordance with the

principles expressed in the Declaration of Helsinki. Thirty-six male, unmedicated veterans aged 18 to 55 years with combat-related PTSD according to the Diagnostic and Statistical Manual of Mental Disorders – Fourth Edition Text Revision (DSM-IV-TR, APA, 2000) participated. Twenty male, combat-exposed, medically and psychiatrically healthy male veterans who did not meet diagnostic criteria of PTSD or any other Axis I psychiatric disorder were also recruited as combat-exposed controls (CEC). Participants, recruited from the community, underwent medical and psychiatric screening evaluations at the Laureate Institute for Brain Research. PTSD diagnoses were determined with the Clinician Administered PTSD Scale (CAPS), which is a gold standard for diagnosing PTSD (Blake et al., 1990, 1995; Weathers et al., 2001), delivered by interviewers trained in the administration of the interviewer. Participants were also administered the Structural Clinical Interview for DSM-IV Disorders, the PTSD Checklist military version (PCL-M; Weathers et al., 1991), Hamilton Anxiety Rating Scale (HARS; Hamilton, 1959), the Snaith-Hamilton Pleasure Scale (SHAPS; Snaith et al., 1995), the Montgomery-Åsberg Depression Rating Scale (MADRS; Montgomery and Åsberg, 1979) and the Hamilton Depression Rating Scale (HDRS; Hamilton, 1960).

Exclusion criteria included general MRI exclusions, psychosis, current or past history of schizophrenia, schizoaffective disorder, bipolar disorder, or dementia, moderate to severe traumatic brain injury, serious suicidal ideation, major medical or neurological disorders, and exposure to any medication likely to influence cerebral function or blood flow within three weeks (eight weeks for fluoxetine), as well as meeting DSM-IV criteria for substance abuse or substance dependence (other than nicotine) within 3 months prior to screening. After receiving a complete explanation of the study procedures, all participants provided written informed consent as approved by the Western Institutional Review Board. Participants received financial compensation for their participation.

2.2. Data acquisition

Simultaneous EEG and fMRI data were acquired in all study participants. MRI scans were completed at the Laureate Institute for Brain Research on General Electric Discovery MR750 whole-body 3 Tesla MRI scanners (GE Healthcare, USA) with standard 8-channel receive-only head coils. Resting-state fMRI data were acquired using a single-shot gradient-recalled EPI sequence with Sensitivity Encoding (SENSE). The resting state session lasts for a total of 8 min and 46 s when participants were instructed to keep their eyes open and fixed on a white cross in front of a gray background. The following EPI imaging parameters were used: FOV/slice = 240/2.9 mm, axial slices per volume = 34, acquisition matrix = 96 × 96, repetition time/echo time (TR/TE) = 2000/30 ms, SENSE acceleration factor R = 2 in the phase encoding (anterior-posterior) direction, flip angle = 90°, sampling bandwidth = 250 kHz. The EPI images were reconstructed into a 128 × 128 matrix, in which the resulting fMRI voxel volume was 1.875 × 1.875 × 2.9 mm³. Additional structural MRI were collected using a T1-weighted magnetization-prepared rapid gradient-echo (MPRAGE) sequence with SENSE. The following parameters were set for structural MRI: FOV = 240 mm, axial slices per slab = 128, slice thickness = 1.2 mm, image matrix = 256 × 256, TR/TE = 5/1.9 ms, acceleration factor R = 2, flip angle = 10°, delay/inversion time TD/TI = 1400/725 ms, sampling bandwidth = 31.2 kHz.

Simultaneous EEG signals were recorded using MRI-compatible BrainAmp MR Plus amplifiers (Brain Products GmbH, Munich, Germany). Thirty-one channels of EEG at the standard 10–20 positions were acquired, with a reference to the FCz position. The electrodes covered the whole brain with an inter-electrode distance of ~5 cm. One additional electrode of electrocardiogram was also acquired for the purpose of correcting the pulse artifacts (Allen et al., 1998). All electrodes were well prepared and maintained with impedance below 10 kΩ throughout the recording. SyncBox device (Brain Products

GmbH, Munich, Germany) was set up for synchronizing the internal sampling clock of the EEG amplifier with the MRI scanner 10 MHz master clock signal for the purpose of removing the gradient artifacts (Allen et al., 2000; Mandelkowitz et al., 2006). The signals were recorded at a sampling frequency of 5000 Hz with an analog filter (from 0.016 to 250 Hz) and a resolution of 0.1 μ V.

Additional auxiliary data included respiration and cardiac pulses recorded by a pneumatic respiration belt and a photoplethysmograph, respectively, for correcting the physiological noise in resting state fMRI data. The recording of the cardiac pulse and respiratory data was synchronized with the fMRI data acquisition. Both waveforms were sampled at a frequency of 50 Hz.

2.3. EEG processing

Preprocessing of the EEG data corrected the artifacts due to simultaneous recording with MRI scanning, i.e. the gradient artifacts and the pulse artifacts, using the average subtraction method (Allen et al., 1998, 2000) implemented in BrainVision Analyzer software (Brain Products GmbH, Munich, Germany). Residual pulse artifacts were removed by using the independent component analysis (ICA) implemented in the EEGLAB toolbox (<http://sccn.ucsd.edu/eeglab/>). In some participants, an EEG channel with extreme noises was disregarded and then interpolated by an average of neighbor channels. The denoised data were subsequently band-pass filtered from 1 Hz to 70 Hz, downsampled to 250 Hz, and re-referenced to the common average reference.

After preprocessing, temporal independent EEG microstates (EEG-ms) were derived using the method described in Yuan et al. (2012). Briefly, the EEG topographies were extracted at the local peaks of global field power, pooled across all sessions and further segregated into temporal independent patterns in a data driven manner by ICA, namely the temporal independent EEG microstates. The number of independent components (ICs) in microstates was chosen to be 30, i.e. the maximum number of channels commonly available among all participants. Components related to nuisance processes (i.e., eye movement, residual pulse artifact and muscle artifact) were further excluded. The temporal independent EEG-ms were separately analyzed for the PTSD and CEC groups. Then the microstates of the PTSD group were matched to each of those in the CEC group by selecting the one with the highest spatial correlation coefficient. A back-projection was performed to obtain time courses associated with each EEG-ms, resulting in continuous time series as the original EEG data. Furthermore, the time series were normalized using a winner-take-all approach, i.e. a microstate was assigned to a time point based on which microstate has the maximal absolute intensity value. The resulted time series of a EEG-ms are composed of series of zeros and ones, with the value of ones at time points when the absolute intensity value of the particular microstate exceeded those of all other microstates. The time course describes the temporal dynamics of the EEG-ms dominating the momentary EEG topographies over other microstates. The occurrence rate of a EEG-ms was calculated as the summation of the time series of the EEG-ms divided by the duration of the period of time, indicating how frequent the EEG-ms dominates the momentary EEG topographies over other microstates.

The occurrence rate of EEG-ms was calculated for each subject, compared across groups, and examined in relation to clinical ratings. Group-level comparison between PTSD and CEC was performed on the occurrence rate of the EEG-ms, using a two-sample, unpaired *t*-test assuming unequal variance.

2.4. fMRI processing

The fMRI data preprocessing was performed using the Analysis of Functional NeuroImages software (AFNI, <http://afni.nimh.nih.gov/>) (Cox, 1996). Preprocessing of the resting state fMRI data steps include

removal of the first five volumes of each run, respiration- and cardiac-induced noise reduction using RETROICOR (Glover et al., 2000), slice timing and rigid-body motion correction, spatial smoothing with a Gaussian kernel (FWHM = 6 mm), and temporal filtering with a bandpass filter (0.01–0.1 Hz). Further processing removed the low-frequency changes in respiration volume and motion as nuisances in the regression (Birn et al., 2006). Spatial co-registration and normalization was conducted by converting fMRI data in the original individual space to a common anatomical space defined in the Talairach and Tournoux template brain (Talairach and Tournoux, 1988) with aid of the Advanced Normalization Tools (<http://www.picsl.upenn.edu/ANTS/>).

After preprocessing, resting state networks of the fMRI were obtained using a spatial ICA implemented in the MELODIC (multivariate exploratory linear optimized decomposition into independent components) tool in the FSL software (Beckmann et al., 2005). The order of independent components (ICs) was determined to be 30, as consistent with EEG and also consistent with other fMRI studies of RSN (Damoiseaux et al., 2006; Smith et al., 2009). The intensity values in each map of each participant were constructed via dual regression (Filippini et al., 2009; Veer et al., 2010), resulting in subject-specific spatial maps of z-scores. Voxel-wise comparison between the PTSD and CEC groups was performed using an unpaired, two-sample *t*-test. The significance criterion for thresholding was set at $p_{\text{corrected}} < 0.05$ determined using the AFNI program 3dClustSim. In addition, an averaged map across all individuals was calculated and thresholded at the value of 2 (Damoiseaux et al., 2006).

2.5. Multi-modal analysis

In order to identify the RSNs associated the EEG-ms, we compared the time courses of the EEG-ms associated with the dynamics of whole-brain fMRI time series. Firstly, to accommodate the dramatically different temporal scales of multimodal EEG and fMRI data, the time courses of the EEG-ms were convolved with a double-gamma hemodynamic response function (HRF) (Friston et al., 1998) and then downsampled to TR, resulting in EEG-ms-informed regressors. The microstate that is related to a resting state network is determined by integrating the EEG-ms-informed regressors in a general linear model (GLM) analysis using a mixed-effect model. EEG-ms-informed statistical maps were created by showing voxels where the time courses of BOLD signals significantly co-varied with the time courses of EEG-ms-informed regressors. The significance criterion for thresholding was set at $p_{\text{corrected}} < 0.05$ determined using the AFNI program 3dClustSim.

The EEG-ms-informed maps were compared with the resting state networks calculated from fMRI. A Pearson's correlation coefficient was calculated between a EEG-ms-informed map and all maps of fMRI RSNs. A particular EEG microstate of interest is associated with a RSN, by selecting and designating the RSN that has the highest spatial correlation with the EEG-ms-informed map. Then the selected fMRI RSNs from our data were compared with 14 template RSNs reported in Shirer et al. (2012). Since the templates were in binary numbers, the selected fMRI RSN maps were thresholded following the procedure described in Shirer et al. (2012). Dice coefficient for a pair of maps in binary values was calculated. An fMRI RSN was labeled with the template RSN that has the highest dice coefficient. Correspondingly, an EEG-informed network matched with the fMRI RSN was also designated with the same label.

3. Results

Thirty-six PTSD veterans and twenty CEC veterans were included in the current analysis. Table 1 lists the demographic and clinical characteristics of the participants of the current study.

A series of ten temporal independent microstates were identified in the groups of PTSD and CEC veterans (Fig. 1). Nine out of the 10 microstates highly resemble those found in our previous study (MS1, MS2,

Table 1
Demographical and clinical characteristics of PTSD group and combat exposed control (CEC) group.

Characteristic	PTSD (n = 36)	CEC (n = 20)
Age (mean ± SD years)	32 ± 7	34 ± 9
PCL-M (mean ± SD) ^{***}	42.9 ± 14.6	18.4 ± 2.2
CAPS (mean ± SD) ^{***}	54.0 ± 18.5	4.7 ± 5.1
SHAPS (mean ± SD) ^{***}	29.9 ± 5.7	23.5 ± 5.8
HARS (mean ± SD) ^{***}	15.3 ± 6.2	2.6 ± 3.5
HDRS (mean ± SD) ^{***}	14.3 ± 5.6	2.6 ± 3.7
MADRS (mean ± SD) ^{***}	17.2 ± 8.2	2.1 ± 3.8

PTSD: post-traumatic stress disorder.

CAPS: Clinician Administered PTSD Scale.

PCL-M: the PTSD Checklist, military version.

HARS: Hamilton Anxiety Rating Scale.

HDRS: Hamilton Depression Rating Scale.

SHAPS: the Snaith-Hamilton Pleasure Scale.

MADRS: the Montgomery-Åsberg Depression Rating Scale.

SD: standard derivation.

^{***} Indicates significant difference between PTSD and HC ($p < 0.001$).

MS4, MS5, MS6, MS7, MS8, MS9 and MS10 in Yuan et al., 2012). Remarkably, the microstates in the current study are obtained from a low-density cap with only 30 EEG channels and from eyes-open resting state. Among the common patterns observed in the healthy participants, the microstates MS1, MS6, MS7, MS8, and MS9 shows patterns in the parietal and occipital cortex. The microstates MS2 and MS4 show strong patterns in the sensorimotor cortex, while microstate MS5 was dominated by temporal-parietal sources. A unique microstate MS11 was identified in the current study, featuring a bilateral pattern with sources originated from the junction of posterior and temporal areas.

As the dynamics of the temporal independent microstates were reconstructed from EEG time series, their signatures at a time scale of millisecond could be examined. Among these EEG-ms, three microstates demonstrated distinctive differences in their fast-evolving dynamics. The EEG-ms that differed between PTSD and CEC groups are marked by dashed lines in Fig. 1. The occurrence rate of these three microstates showed significant difference between groups. For microstates MS1 and MS11, the PTSD group showed significantly higher occurrence rate than the control group, whereas for microstate MS 10, the PTSD group showed a lower occurrence rate. All other microstates failed to demonstrate group-level difference between PTSD and CEC in terms of their occurrence rate.

To further explore the neuronal substrates of these three signature microstates, the temporal dynamics of the microstate were compared with the time courses of BOLD signals after convolving with the impulse hemodynamic response function. Regions where BOLD and EEG microstate time series are correlated were identified using a general linear model, resulting in EEG-ms-informed networks. The EEG-informed networks were then compared with the resting state network calculated

from fMRI data. The selected fMRI RSN from our data were further compared with 14 template RSN from Shirer et al. (2012). The fMRI RSN and their corresponding EEG-ms-informed network were designated with the same label of best-matched template RSN. The dorsal default model network (dDMN) was therefore identified associated with one of the EEG microstates, MS1 (Fig. 2). Importantly, the occurrence rate of the dDMN-associated EEG microstates shows distinctive temporal dynamics between CEC and PTSD groups (i.e., higher in the PTSD group). Moreover, the occurrence rate of the EEG-ms was also linearly related to the scores of PCL-M scores in the PTSD group, indicating that more severe PTSD symptoms are associated with higher occurrence rate of the dDMN network. While functional MRI was able to pinpoint the anatomical regions of DMN, simultaneous EEG offers fast temporal dynamics that facilitate relating them to the severity of symptoms. Regarding dorsal DMN, the comparison between the fMRI RSN found in our data and the template RSN is shown in Supplemental Fig. S1.

Two other microstates MS 10 and MS11, were also found to be associated with distinctive dynamics between PTSD and CEC groups. Interestingly, both MS10 and MS11 identified a similar network, involving bilateral insular, the cingulate cortex and the medial temporal cortex. As outcomes of the matching procedure, MS10 (Fig. 3) appears to engage the anterior salience network (aSN) that includes the anterior insular, dorsal anterior cingulate/paracingulate cortex, and the medial thalamus. Meanwhile, MS11 (Fig. 4) is related to the posterior salience network (pSN) that includes the posterior insular region and dorsal anterior cingulate cortex. However, the temporal dynamics of MS10 and MS11 show importantly different characteristics. For MS11 (related to aSN), the PTSD group showed significantly higher occurrence rate than the control group, whereas for microstate MS 10 (related to pSN), the PTSD group showed lower occurrence rate. Furthermore, the dynamics of MS10 was found to negatively correlate with SHAPS scores across the individual subjects, which assess hedonic experience or positive valence. Therefore, in the PTSD group, participants with higher level of hedonic tone are associated with lower occurrence rate of the anterior salience network. The dynamics of MS11 did not show any significant linear trend between the occurrence rate and the level of symptoms ($p > 0.05$ for both PCL-M and SHAPS scores). For anterior and posterior salience networks, the comparison between the fMRI RSN found in our data and the template RSN is shown in Supplemental Figs. S2 and S3.

Furthermore, our analysis evaluated the group-level difference in the three fMRI RSNs between PTSD and CEC. Using similar statistical criteria for thresholding the EEG-ms-informed networks, no regions with significant difference between PTSD and CEC groups were identified in the fMRI RSN maps (Supplemental Figures S1-S3). To illustrate the comparison, representative images of the group mean for PTSD and CEC are shown in Supplemental Fig. S4.

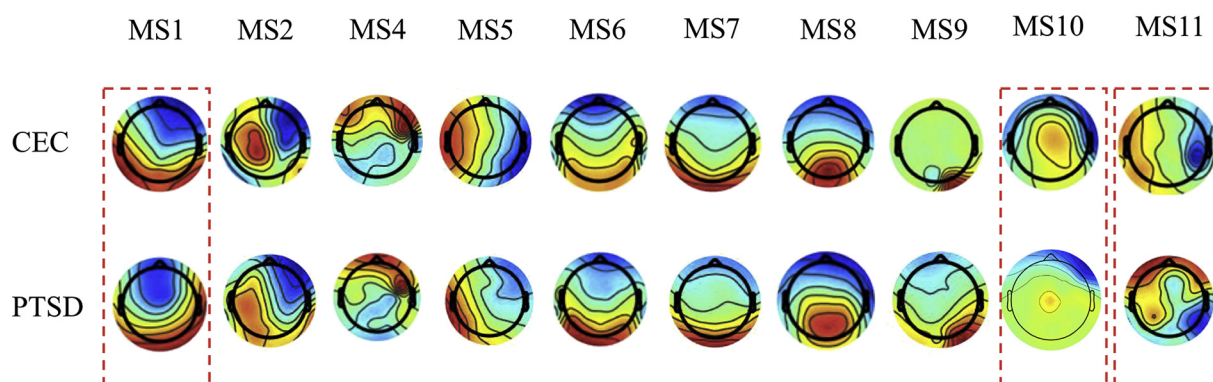


Fig. 1. Microstates identified in CEC and PTSD groups. The pairs of microstates in dashed lines show distinct features between CEC and PTSD groups.

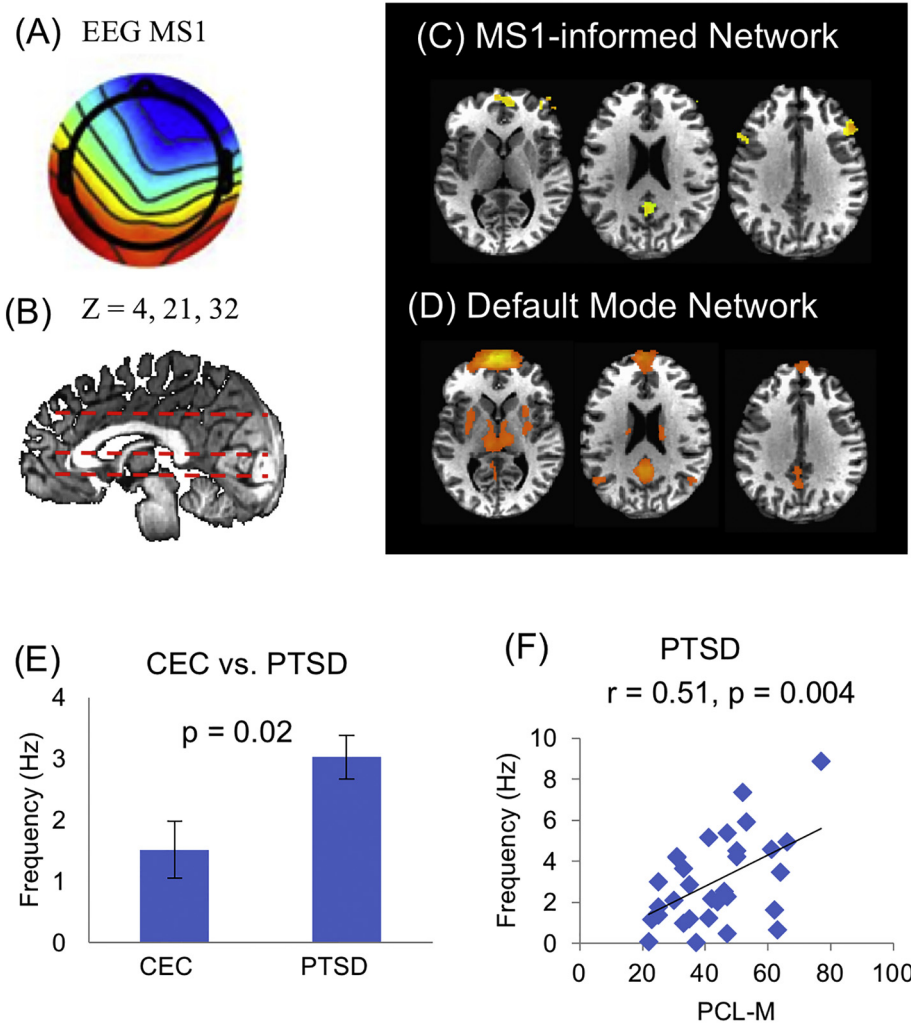


Fig. 2. Dorsal default mode network. Analysis of temporal dynamics identified that microstate MS1 (A) is related to an EEG-informed network (C) which resembles the fMRI dorsal default mode network (D), showing at positions $z = 4, 21$ and 32 (B). (E) Occurrence rate of microstate MS1 differs between CEC and PTSD groups ($p = 0.02$). (F) In all thirty-six PTSD individuals, the occurrence rate of microstate MS1 is positively correlated to the score of symptom severity measured by PCL-M ($r = 0.51, p = 0.004$).

4. Discussions

We investigated and compared the electrophysiological signatures of hemodynamic RSNs in male veterans with and without combat related PTSD. To our knowledge, this is the first examination of resting state networks in PTSD using a multimodal concurrent EEG-fMRI approach and also controls for combat exposure. We proposed a new strategy to integrate EEG and fMRI by quantifying the fast temporal dynamics associated with the resting state networks as the occurrence rate of EEG-ms. Results show that in three fMRI derived resting state networks, namely dorsal DMN as well as anterior and posterior SNs networks, the temporal dynamics characterized and measured by EEG, differ as a function of PTSD. The electrophysiological correlates – temporal independent EEG microstates associated with the DMN and anterior and posterior SNs – show aberrant occurrence rate in PTSD. In particular, the occurrence rate of the DMN is higher in PTSD and positively correlated with the score of PTSD severity. In contrast, the occurrence rate of the anterior SN is lower in PTSD and negatively correlated with the score of hedonic tone or degree of pleasantness.

Multiple brain regions have been depicted in the imaging studies of PTSD, as patterns of activations during tasks of symptom provocation. Hyperactivity of limbic brain regions (e.g., amygdala, insula) and hypoactivity of brain areas involved in emotional regulation (e.g.,

ventromedial prefrontal cortex [vmPFC], dorsal anterior cingulate cortex [dACC]) have been observed, suggesting insufficient top-down modulation of limbic regions (especially the amygdala) by the prefrontal cortex (Rauch et al., 2006; Liberzon and Sripada, 2007; Pitman et al., 2012). In addition, fMRI imaging of RSFC or RSN has become a useful tool in the investigation of the neurobiological mechanism of PTSD, as the disease shows symptoms of re-experiencing the traumatic events, avoidance and hyperarousal at resting state. Patterns of connectivity between the PTSD-implicated regions could give new information on the neural basis of PTSD, and on mechanisms of PTSD symptom development. The connectivity studied at resting-state provides new and complementary knowledge to the connectivity imaged at task conditions (Hayes et al., 2011; Dahlgren et al., 2017; Daniels et al., 2010).

Multimodal imaging using simultaneous EEG and fMRI has been recently exploited in studying the mechanisms or functions of the RSNs in the human brain (Mantini et al., 2007; Britz et al., 2010; Musso et al., 2010; Deco et al., 2011; Yuan et al., 2012). The simultaneously acquired EEG data provides high-temporal resolution to capture the millisecond-level recordings of neural activity (Yuan et al., 2011, 2012, 2016), physiological noise (Yuan et al., 2013), or head movement (Zotev et al., 2012; Wong et al., 2016). The temporal independent EEG-ms (Yuan et al., 2012) have been discovered and shown to be coupled

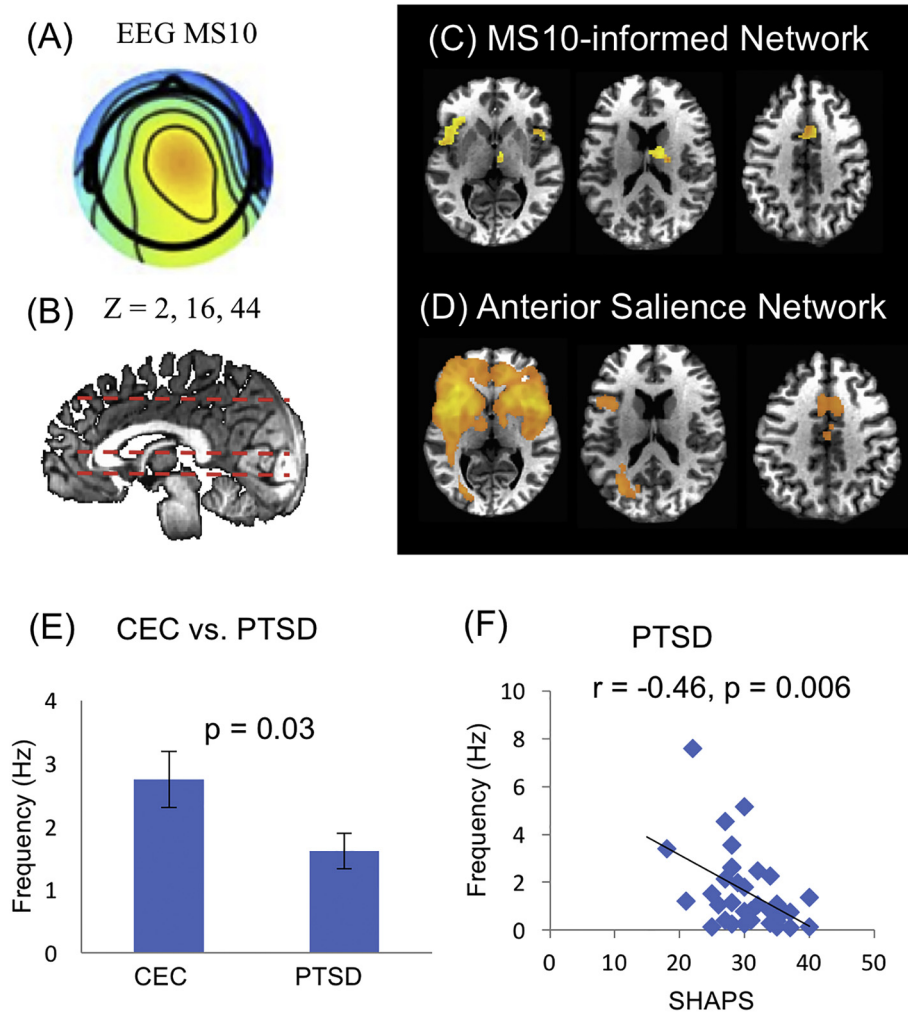


Fig. 3. Anterior salience network. Analysis of temporal dynamics identified that microstate MS10 (A) is related to an EEG-informed network (C) which resembles the fMRI anterior salience network (D), showing at positions $z = 2, 16$ and 44 (B). (C) Occurrence rate of microstate MS10 differs between CEC and PTSD groups ($p = 0.03$). (D) In the PTSD individuals, the occurrence rate of microstate MS10 is inversely correlated to the score of hedonic tone measured by the Snaith-Hamilton Pleasure Scale (SHAPS) ($r = -0.46, p = 0.006$).

to the temporal dynamics of BOLD RSNs. More intriguingly, the source generators of the temporal independent EEG microstates have been reconstructed using EEG source imaging and shown to spatially match eight of the resting state networks established in fMRI studies (Yuan et al., 2016). Taken together, the temporal independent EEG-ms are electrophysiological correlates to specific resting state networks, both in their spatial patterns and temporal dynamics. In our current study, we capitalize on the rich temporal information obtained from the EEG and investigate how PTSD relates to temporal electrophysiological signatures in two hemodynamic RSNs of interest, the DMN and the SN.

Our investigations based on simultaneous EEG and fMRI data revealed novel findings about the temporal dynamics of the DMN by comparing veterans with war-related PTSD and combat-exposed veterans without PTSD diagnosis as controls. Particularly, we have taken a novel approach of quantifying the temporal dynamics of DMN as the occurrence rate of the EEG-ms associated with DMN. The EEG microstate MS1 was observed to be associated with dorsal DMN, as its temporal dynamics were found to be related to the fluctuating activities from regions including the precuneus, the medial prefrontal gyrus (MPFC) and the bilateral dorsal lateral PFC, which constitutes the key nodes of the DMN (Buckner et al., 2008). The precuneus is involved in autobiographical memory and is also related to self-referential processing (Lou et al., 2004; Cavanna and Trimble, 2006; Yuan et al., 2014). Furthermore, precuneus activity has been related to trauma memory

generalization (Hayes et al., 2011), and flashbacks (Whalley et al., 2013). Thus, alterations in the precuneus are associated with PTSD and may potentially be related to altered memory- and self-referential processes in PTSD, such as memory deficits, intrusions or flashbacks (Kessler, 2000; Etkin and Wager, 2007). Our results showed increased occurrence rate of DMN-related electrophysiological states in the veterans with PTSD, which indicates increased temporal dynamics of the DMN, as compared to trauma-exposed veteran controls. As one occurrence of a specific EEG-ms represents a dominating transient state of the brain activities, the increased occurrence rate of the DMN-associated microstates suggests that DMN activities in regions related with memory and self-referential processing exhibit abnormal hyper frequency as dominating transient moments. More importantly, the occurrence rates across all PTSD individuals showed a significant positive correlation with the PCL-M scores, with severer PTSD symptoms associated with higher occurrence rate of the DMN-associated EEG-ms activities. This association suggests the potential of using the occurrence rate of electrophysiological states (e.g. EEG-microstates) derived from simultaneous EEG-fMRI as a biomarker of PTSD symptom severity. Our results are consistent with notion that the DMN activity is disturbed in PTSD, with more DMN activity presence in ongoing brain activity, and provide independent neurophysiological evidences for abnormalities in processing emotions and memory information.

In addition, a number of studies have used resting-state fMRI to

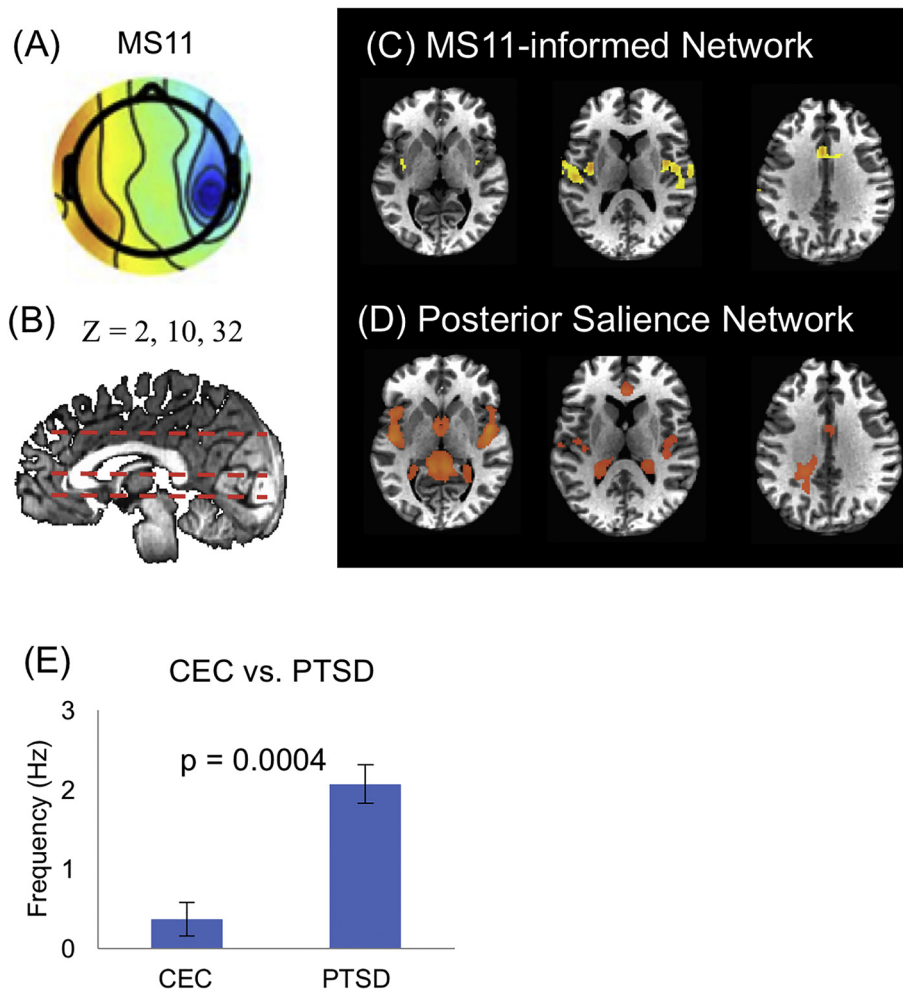


Fig. 4. Posterior salience network. Analysis of temporal dynamics identified that microstate MS11 (A) is related to an EEG-informed network (C) which resembles the fMRI posterior salience network (D), showing at positions $z = 2, 10$ and 32 (B). (C) Occurrence rate of microstate MS11 significantly differs between CEC and PTSD groups ($p = 0.0004$). Among the PTSD individuals, neither the score of PTSD severity nor the score of hedonic tone was correlated with the occurrence rate of microstate MS11.

investigate the connectivity in PTSD. During rest, disrupted connectivity within the DMN has been reported in PTSD due to early-life traumatic events (Bluhm et al., 2009; Daniels et al., 2011) and the related psychiatric problem of acute stress disorder (Lui et al., 2009; Lanius et al., 2010), which were all related to civilian trauma. Others, in the meantime, used resting state fMRI to study the effect of combat-related trauma by examining network-level alternations of DMN in combat-related PTSD (Miller et al., 2017; Kennis et al., 2015a,b; Yan et al., 2013; Koch et al., 2016; DiGangi et al., 2016; Sripada et al., 2012a; Misaki et al., 2017). For example, Sripada et al. (2012a) reported that PTSD veteran participants showed reduced functional connectivity within DMN (including both the poster and dorsal DMN), as compared to a combination of combat-exposed controls and healthy community controls. Such reduced DMN connectivity in combat-related PTSD (Sripada et al., 2012a) is consistent with the finding of reduced DMN connectivity in PTSD related to early-life trauma (Bluhm et al., 2009). However, in the study of combat-related PTSD, the way of using civilians as control (DiGangi et al., 2016; Misaki et al., 2017) or a combined cohort of combat and civilian controls (Koch et al., 2016; Kennis et al., 2015a; Sripada et al., 2012a) raises important concerns of whether the observed difference is evident in comparison to combat exposed veterans without PTSD, or just to the healthy civilians. In this regard, a study by DiGangi et al. (2016) explicitly examined details of DMN connectivity in three groups: veterans with combat-related PTSD, combat-exposed controls without PTSD and never-traumatized healthy

controls and compared their resting state functional connectivity. As compared to a cohort of healthy civilians reduced DMN connectivity was observed in the group of veterans with PTSD as well as the group of veterans without PTSD. However, when contrasting the group of PTSD veterans to the group of veterans without PTSD, difference in DMN associated with PTSD was not evident. Thus, it remains unclear whether the abnormality of resting state networks is due to the experience of trauma, or the pathology of PTSD. Another independent study by Kennis et al. (2015a,b) investigated different parts of ACC, and found out specific difference in connectivity between veterans with combat-related PTSD and combat exposed controls. In the connectivity with regard to the perigenual ACC (pgACC; i.e. part of the dorsal DMN), *no difference* was found between PTSD veterans and combat exposed controls; whereas as compared to the healthy controls, both veteran groups with and without PTSD showed reduced functional connectivity between pgACC and the supramarginal gyrus (SMG) and middle temporal gyrus (MTG) with regard to the pgACC, which are all parts of the DMN. Similarly, our study using a combat-exposed control did not reveal difference in DMN connectivity in PTSD at a comparable sample size with Kennis et al. (2015a,b). Likewise, Misaki et al. (2017) did not reveal difference in DMN connectivity when comparing the PTSD veterans and trauma-exposed control veterans. More recently, however, in a large-sample study that recruited 69 participants with combat PTSD and 44 trauma-exposed controls (Miller et al., 2017), the disrupted connectivity in DMN was reported. Reduced connectivity was observed

between posterior cingulate cortex and hippocampus, which both are key regions of the DMN, in the PTSD group as compared to trauma-exposed controls. Nonetheless, it still remains unclear to what level does the connectivity in the dorsal regions of DMN differs between combat PTSD and combat-exposed control, particularly in the dorsal medial prefrontal cortex (MPFC) region that is essentially engaged in the dysregulation of attention, memory and emotion (Sheline et al., 2010). Although our study did not reveal any group-level difference in the connectivity of DMN in PTSD as compared to the combat exposed controls, our results of the DMN-associated EEG-ms add novel information regarding the temporal dynamics of the dorsal DMN including the regions of PCC and MPFC.

Noteworthy, however, the increased temporal dynamics of DMN as observed using simultaneous EEG-fMRI data do not equal increased connectivity in DMN as obtained using fMRI data alone. Our novel results provide complementary information to the existing literature about neural networks implicated in PTSD. We found significant difference in the occurrence rate of DMN-related microstates in PTSD, although the fMRI connectivity analysis using a data-driven, spatial ICA approach did not reveal any difference in the connectivity strength of DMN that was significant in the PTSD group as compared with the combat-exposed controls. The two metrics, fMRI-based connectivity of a RSN and occurrence rate of a RSN-associated EEG-ms, capture different properties of a network. The fMRI connectivity is calculated based on the temporal correlation between the fluctuating activities measured by fMRI, which captures the within-network property. Thus, higher strengths of fMRI connectivity within a RSN indicate a strong synchronization in the ups and downs of momentary activities between regions within a RSN. In the contrary, the occurrence rate of a RSN-associated microstate describes the between-network property, the frequency regarding the dominance of a RSN in the momentary states of brain activities. Higher occurrence rate of a RSN-associated microstate indicates higher frequency of dominance for the RSN, which suggests a strong presence of the RSN against other RSNs. The two metrics provide complementary information about the within- and between-network properties of a RSN. Particularly, the approach of characterizing the temporal dynamics of RSN used in the current study is novel. Future investigations are warranted to further understand the occurrence rate as a between-network characterization and its relationship with other literature on the fMRI connectivity.

In addition to the DMN, the salience network (Seeley et al., 2007) has been another focus in the neuroimaging studies of PTSD, including our current study. The SN consists of dorsal anterior cingulate (dACC) and orbital frontoinsula cortices with robust connectivity to sub-cortical and limbic structures. Further delineation of the salience network resulted in two sub-networks, the anterior SN and the posterior SN (Shirer et al., 2012). Studies of SN have suggested its role in detecting and orienting to salient stimuli (Dosenbach et al., 2007; Sridharan et al., 2008), emotional control (Seeley et al., 2007), cognitive control (Menon and Uddin, 2010), and error processing (Ham et al., 2013). In particular, the intrinsic functional connectivity of the dACC node of the SN has been associated with anxiety ratings in the healthy population (Seeley et al., 2007). Alterations in the SN that are associated with PTSD, however, have been investigated in a limited number of studies. The insula and amygdala have been found to be hyperactive in PTSD (Shin and Liberzon, 2010; Etkin and Wager, 2007) and are involved in the SN (Cauda et al., 2011). Reduced ACC resting state functional connectivity with the thalamus, amygdala, posterior cingulate cortex (PCC)/precuneus, and prefrontal regions has been reported in PTSD versus non-trauma-exposed controls (Kennis et al., 2015a,b; Daniels et al., 2010), trauma-exposed controls (Sripada et al., 2012b; Yan et al., 2013; Rabinak et al., 2011; Misaki et al., 2017) or both (Kennis et al., 2015a; Sripada et al., 2012a). In a recent study, Misaki et al. (2017) conducted data-driven, connectome-wide investigation of altered resting-state functional connectivity for war veterans with PTSD and without PTSD diagnosis, and age-match matched healthy male civilian

controls, revealed hypo-connectivity between the parahippocampal gyrus and the visual cortex as well as across the lateral prefrontal and vmPFC with the SN regions. PTSD symptom severity was negatively correlated with connectivity between the right parahippocampal gyrus and the right anterior insula and between the left vmPFC and the left middle frontal gyrus. These alterations were consistent with previous observations of abnormalities in the emotion-regulation circuit and further support dissociated memory representation in PTSD. The authors also report increased connectivity with posterior insula and decreased connectivity with precuneus among veterans without PTSD, with the later suggesting adaptive alteration to suppress traumatic memory. However, no significant differences in resting-state functional connectivity between the veterans with PTSD and without PTSD diagnosis was found, although significant connectivity decrease with DMN in veterans without PTSD diagnosis was reported (Misaki et al., 2017). As discussed above, using a control group of non-trauma-exposed civilian or a combination of combat-exposed and non-combat-exposed controls raises methodological concerns and may limit the interpretation of the findings. In this regard, Kennis et al. (2015a,b) explicitly investigated how the choice of control group could impact pattern of SN seeded at the dorsal ACC cortex, and found out no difference exist between veterans with combat-related PTSD and combat exposed controls, which yielded similar findings by Misaki et al. (2017) using a completely data-drive approach.

Our results found distinct PTSD-related signatures for the anterior SN and the posterior SN, as compared with trauma-exposed veteran controls. The microstate MS10 was observed to be the electrophysiological correlate of the anterior SN, which includes the anterior insular, dorsal anterior cingulate/paracingulate cortex, and the medial thalamus. In contrast, MS11 is related to the posterior salience network that includes the posterior insular region and dACC. The delineation of anterior and posterior SN has been documented in data-driven studies of resting-state fMRI data (Shirer et al., 2012) and tractography-based studies of diffusion tensor imaging data (Figley et al., 2015). However, the functional relevance of the subnetworks of the SN is not yet fully delineated. Our study compared the temporal dynamics of the EEG microstates associated with the anterior and posterior SN: *decreased* temporal dynamics in the anterior SN, yet *increased* dynamics in the posterior SN, were observed in PTSD. These results suggest an antagonist relationship between the anterior and posterior SN in PTSD. More interestingly, the dynamics of the anterior SN is related to the hedonic tone of the participants. The PTSD group was found to have significantly higher hedonic tone than the controls, and correspondingly the PTSD participants show a significantly lower occurrence rate EEG-ms associated with anterior SN. In line with the group-level finding, at an individual level in the PTSD group, the higher the score of hedonic tone is, the less frequently the anterior SN EEG-ms occurs. These results suggest that activity of the SN is disturbed in people with PTSD while at rest, and are consistent with work documenting abnormal functioning of the emotion regulation network in this population.

Moreover, the SN is thought to play a critical role modulating and regulating the balance between DMN and central-executive network (CEN) activity (Sridharan et al., 2008; Bressler and Menon, 2010). Sripada et al. (2012a) showed antagonist features of disruption in SN and DMN in combat-related PTSD, i.e. reduced coupling within DMN was accompanied by increased coupling within SN and increased coupling between DMN and SN. However, a mixture of combat exposed control and civilian controls were used in the study by Sripada et al. (2012a), which could not attribute the findings to the factor of combat trauma exposure. In the contrary, by comparing the PTSD individuals to the combat exposed controls, our study found that the temporal dynamics of DMN and SN derived from EEG data concurrently recorded during fMRI show antagonist features. Whereas the temporal dynamics of DMN become more frequently dominant in PTSD, the states of the anterior SN go in an opposite, diminishing direction. Interestingly, the

exaggerated DMN dynamics are positively associated with the severity of PTSD symptoms whereas the diminishing states of the anterior SN are negatively associated with the hedonic tone across PTSD individuals. Moreover, the posterior SN has been also delineated in our findings. Although the states of the posterior SN show higher occurrence rate in the PTSD than the CEC group, it remains still unclear about the functional underpinning of the posterior SN.

Our results demonstrate the merit of multimodal imaging in studying the neural mechanism of PTSD. The current results confirmed our previous findings that temporal independent microstates are electrophysiological correlates of distinct RSNs, as shown here in two independent cohorts of adult participants (combat-exposed healthy males without, and males with combat-related PTSD). We provided novel evidence that temporal dynamics of large-scale DMN and SNs, reflected by EEG-ms associated with these networks, differentiate the PTSD and combat-exposed controls groups. By relating to other studies on EEG microstate (Lehmann et al., 1987; Koenig et al., 2002), we have previously proposed that these miniature brain states of temporal independent EEG microstates represent putative neuronal events in the form of spatially and temporally synchronized neuronal activity (Yuan et al., 2016). The spontaneous brain network activity may be driven by synchronized burst-type neural events (~40 ms, EEG-ms physiologically relevant time scale), which can be separated into temporally independent processes representing functional RSNs. In such a framework, the EEG-ms and RSNs may refer to the common building blocks of brain spontaneous neuronal activity. More importantly, the concept of the microstate introduces new ways to dictate the dynamics of resting state brain activity (Khanna et al., 2015). The temporal dynamics of EEG microstates, such as occurrence rate or duration of states, are found to be altered in panic disorder (Kikuchi et al., 2011), schizophrenia (Kindler et al., 2011), and dementia (Nishida et al., 2013; Hatz et al., 2015; Grieder et al., 2016). Here, our results documented that temporal independent EEG microstates associated with DMN and SNs are altered in combat-related PTSD.

Our findings revealed that the temporal dynamics of the DMN- and SN-associated EEG-ms are associated with PTSD severity and hedonic tone, respectively, suggest that such neuroimaging metrics may be used as PTSD-related biomarkers. While future investigations on such neuroimaging metrics are warranted to fully characterize their relevance to psychopathology of PTSD, and to clinically relevant outcome measures, EEG-ms have potentials in facilitating the diagnosis and prognosis of PTSD. Furthermore, since EEG-ms is related to the level of disease severity, it may be used as an evaluation biomarker in determining the effectiveness of an intervention or treatment. A relevant work from our group showed that the EEG microstates exploited in the current study can also be constructed from EEG alone data (Yuan et al., 2016). The temporal independent microstates based on stand-alone EEG data may be able to provide more portable and less expensive way for researching novel interventions for PTSD. Another potential use of EEG-ms is as neurofeedback training for user to alleviate the symptom via a learning by biofeedback approach (Zotev et al., 2014). Since instrumentation for EEG-based neurofeedback is considerably affordable and portable, it opens another avenue of use for the EEG-ms.

5. Conclusion

Our study employed a novel approach to study the fast dynamics of resting state networks associated with PTSD by using simultaneous EEG and fMRI. To our knowledge, this study for the first time showed differences in the fast temporal dynamics of dorsal default mode network, anterior and posterior salience networks, comparing veterans with combat-related PTSD to combat-exposed veteran controls without PTSD. The occurrence rate of the EEG microstates associated with the dorsal default mode network was higher in PTSD than control, and positively associated with the severity of PTSD symptoms. The occurrence rate of the electrophysiological state associated with the anterior

salience network was lower in PTSD than control, and negatively associated with the hedonic tone in PTSD participants. Our findings contribute new information to our understanding of the neural mechanisms of PTSD, and further suggest that a disruption in emotion generation and regulation circuits plays a crucial role and contributes to the pathophysiology of PTSD. Moreover, the study suggests that multimodal neuroimaging yields valuable information about large-scale neural activity in high temporal resolution and high spatial resolution and is a useful technology for understanding neuropsychiatric disorders.

Acknowledgements

This work was supported by the W81XWH-12-1-0697 grant from the U.S. Department of Defense. The authors thank all staff members at Laureate Institute for Brain Research, Matthew Meyer, M.D., and William Yates, M.D. for conducting psychiatric interviews, Tim Collins, Lisa Kinyon, and Megan Cole for administering clinical interviews and assessments, and Julie Owen, Julie Crawford, Leslie Walker, and Tressia Lewis for helping with MRI scanning. The funding agencies were not involved in the design of experiment, data collection and analysis, interpretation of results and preparation and submission of the manuscript. The authors declare that they have no conflict of financial interest.

Appendix A. Supplementary data

Supplementary data to this article can be found online at <https://doi.org/10.1016/j.nicl.2018.04.014>.

References

- Allen, P.J., Polizzi, G., Krakow, K., Fish, D.R., Lemieux, L., 1998. Identification of EEG events in the MR scanner: the problem of pulse artifact and a method for its subtraction. *NeuroImage* 8, 229–239.
- Allen, P.J., Josephs, O., Turner, R., 2000. A method for removing imaging artifact from continuous EEG recorded during functional MRI. *NeuroImage* 12, 230–239.
- American Psychiatric Association, 2000. *Diagnostic and Statistical Manual of Mental Disorders, 4th Ed. Text Revision (DSM-IV-TR)*. American Psychiatric Press, Washington, DC.
- American Psychiatric Association, 2013. *Diagnostic and Statistical Manual of Mental Disorders, 5th Ed. (DSM-5)*. American Psychiatric Press, Washington, DC.
- Beckmann, C.F., DeLuca, M., Devlin, J.T., Smith, S.M., 2005. Investigations into resting-state connectivity using independent component analysis. *Philos. Trans. R. Soc. Lond. Ser. B Biol. Sci.* 360, 1001–1013.
- Birn, R.M., Diamond, J.B., Smith, M.A., Bandettini, P.A., 2006. Separating respiratory-variation-related fluctuations from neuronal-activity-related fluctuations in fMRI. *NeuroImage* 31, 1536–1548.
- Biswal, B., Yetkin, F.Z., Haughton, V.M., Hyde, J.S., 1995. Functional connectivity in the motor cortex of resting human brain using echo-planar MRI. *Magn. Reson. Med.* 34, 537–541.
- Blake, D.D., Weathers, F.W., Nagy, L.M., Kaloupek, D.G., Klauminzer, G., Charney, D.S., Keane, T.M., 1990. A clinician rating scale for assessing current and lifetime PTSD: the CAPS-1. *Behav. Ther.* 13, 187–188.
- Blake, D., Weathers, F., Nagy, L., Kaloupek, D., Gusman, F., Charney, D., Keane, T., 1995. The development of a clinician-administered PTSD scale. *J. Trauma. Stress.* 8, 75–90.
- Bluhm, R.L., Williamson, P.C., Osuch, E.A., Frewen, P.A., Stevens, T.K., Boksman, K., Neufeld, R.W., Théberge, J., Lanius, R.A., 2009. Alterations in default mode network connectivity in posttraumatic stress disorder related to early-life trauma. *J. Psychiatry Neurosci.* 34 (3), 187–194.
- Bressler, S.L., Menon, V., 2010. Large-scale brain networks in cognition: emerging methods and principles. *Trends Cogn. Sci.* 14, 277–290.
- Britz, J., Van De Ville, D., Michel, C.M., 2010. BOLD correlates of EEG topography reveal rapid-state network dynamics. *NeuroImage* 52 (4), 1162–1170.
- Brown, V.M., LaBar, K.S., Haswell, C.C., Gold, A.L., Mid-Atlantic MIRECC Workgroup, McCarthey, G., Morey, R.A., 2014. Altered resting-state functional connectivity of basolateral and centromedial amygdala complexes in posttraumatic stress disorder. *Neuropsychopharmacology* 39 (2), 351–359.
- Buckner, R.L., Andrews-Hanna, J.R., Schacter, D.L., 2008. The brain default network: anatomy, function, and relevance to disease. *Ann. N. Y. Acad. Sci.* 1124, 1–38.
- Cauda, F., D'Agata, F., Sacco, K., Duca, S., Geminiani, G., Vercelli, A., 2011. Functional connectivity of the insula in the resting brain. *NeuroImage* 55, 8–23.
- Cavanna, A.E., Trimble, M.R., 2006. The precuneus: a review of its functional anatomy and behavioural correlates. *Brain* 129 (3), 564–583.
- Cox, R.W., 1996. AFNI: software for analysis and visualization of functional magnetic resonance neuroimages. *Comput. Biomed. Res.* 29, 162–173.

- Dahlgren, M.K., Laifer, L.M., VanElzakker, M.B., Offringa, R., Hughes, K.C., Staples-Bradley, L.K., Dubois, S.J., Lasko, N.B., Hinojosa, C.A., Orr, S.P., Pitman, R.K., Shin, L.M., 2017. Diminished medial prefrontal cortex activation during the recollection of stressful events in an acquired characteristic of PTSD. *Psychol. Med.* 12, 1–13.
- Damoiseaux, J.S., Rombouts, S.A., Barkhof, F., Scheltens, P., Stam, C.J., Smith, S.M., Beckmann, C.F., 2006. Consistent resting-state networks across healthy subjects. *Proc. Natl. Acad. Sci.* 103, 13848–13853.
- Daniels, J.K., McFarlane, A.C., Bluhm, R.L., Moores, K.A., Clark, G.R., Shawn, M.E., Williamson, P.C., Densmore, M., Lanius, R.A., 2010. Switching between executive and default mode networks in posttraumatic stress disorders: alterations in functional connectivity. *J. Psychiatry Neurosci.* 35 (4), 258–266.
- Daniels, J.K., Frewen, P., McKinnon, M.C., Lanius, R.A., 2011. Default mode alterations in posttraumatic stress disorder related to early-life trauma: a developmental perspective. *J. Psychiatry Neurosci.* 36, 56–59.
- Deco, G., Jirsa, V.K., McIntosh, A.R., 2011. Emerging concepts for the dynamical organization of resting-state activity in the brain. *Nat. Rev. Neurosci.* 12 (1), 43–56.
- DiGangi, J.A., Tadayyon, A., Fitzgerald, D.A., Rabinak, C.A., Kennedy, A., Klumpp, H., Rauch, S.A., Phan, K.L., 2016. Reduced default mode network connectivity following trauma. *Neurosci. Lett.* 615, 37–43.
- Dosenbach, N.U., Fair, D.A., Miezin, F.M., Cohen, A.L., Wenger, K.K., Dosenbach, R.A., Fox, M.D., Snyder, A.Z., Vincent, J.L., Raichle, M.E., Schlaggar, B.L., Petersen, S.E., 2007. Distinct brain networks for adaptive and stable task control in humans. *Proc. Natl. Acad. Sci. U. S. A.* 104, 11073–11078.
- Etkin, A., Wager, T.D., 2007. Functional neuroimaging of anxiety: a meta-analysis of emotional processing in PTSD, social anxiety disorder, and specific phobia. *Am. J. Psychiatry* 164, 1476–1488.
- Figley, T.D., Bhullar, N., Courtney, S.M., Figley, C.R., 2015. Probabilistic atlases of default mode, executive control and salience network white matter tracts: an fMRI-guided diffusion tensor imaging and tractography study. *Front. Hum. Neurosci.* 9, 585.
- Filippini, N., MacIntosh, B.J., Hough, M.G., Goodwin, G.M., Frisoni, G.B., Smith, S.M., Matthews, P.M., Beckmann, C.F., Mackay, C.E., 2009. Distinct patterns of brain activity in young carriers of the APOE-epsilon4 allele. *Proc. Natl. Acad. Sci. U. S. A.* 106, 7209–7214.
- Fox, M.D., Raichle, M.E., 2007. Spontaneous fluctuations in brain activity observed with functional magnetic resonance imaging. *Nat. Rev. Neurosci.* 8, 700–711.
- Friston, K.J., Fletcher, P., Josephs, O., Holmes, A., Rugg, M.D., Turner, R., 1998. Event-related fMRI: characterizing differential responses. *NeuroImage* 7, 30–40.
- Glover, G.H., Li, T.Q., Ress, D., 2000. Image-based method for retrospective correction of physiological motion effects in fMRI: RETROICOR. *Magn. Reson. Med.* 44, 162–167.
- Greicius, M.D., Supekar, K., Menon, V., Dougherty, R.F., 2009. Resting-state functional connectivity reflects structural connectivity in the default mode network. *Cereb. Cortex* 19 (1), 72–78.
- Grieder, M., Koenig, T., Kinoshita, T., Utsunomiya, K., Wahlund, L.O., Dierks, T., Nishida, K., 2016 May. Discovering EEG resting state alterations of semantic dementia. *Clin. Neurophysiol.* 127 (5), 2175–2181.
- Ham, T., Leff, A., de Boissezon, X., Joffe, A., Sharp, D.J., 2013. Cognitive control and the salience network: an investigation of error processing and effective connectivity. *J. Neurosci.* 33, 7091–7098.
- Hamilton, M., 1959. The assessment of anxiety states by rating. *Br. J. Med. Psychol.* 32, 50–55.
- Hamilton, M., 1960. A rating scale for depression. *J. Neurol. Neurosurg. Psychiatry* 23, 56–62.
- Hatz, F., Hardmeier, M., Benz, N., Ehrensperger, M., Gschwandtner, U., Ruegg, S., Schindler, C., Monsch, A.U., Fuhr, P., 2015. Microstate connectivity alterations in patients with early Alzheimer's disease. *Alzheimers Res. Ther.* 7, 78 (Dec 31).
- Hayes, J.P., LaBar, K.S., McCarthy, G., Selgrade, E., Nasser, J., Dolcos, F., Morey, R.A., 2011. Reduced hippocampal and amygdala activity predicts memory distortions for trauma reminders in combat-related PTSD. *J. Psychiatr. Res.* 45 (5), 660–669.
- He, B.J., Snyder, A.Z., Zempel, J.M., Smyth, M.D., Raichle, M.E., 2008. Electrophysiological correlates of the brain's intrinsic large-scale functional architecture. *Proc. Natl. Acad. Sci.* 105, 16039–16044.
- Hoge, C.W., Castro, C.A., Messer, S.C., McGurk, D., Cotting, D.I., Koffman, R.L., 2004. Combat duty in Iraq and Afghanistan, mental health problems, and barriers to care. *N. Engl. J. Med.* 351, 13–22.
- Kennis, M., van Rooij, S.J., van den Heuvel, M.P., Kahn, R.S., Geuze, E., 2015a. Functional network topology associated with posttraumatic stress disorder in veterans. *NeuroImage Clin.* 10, 302–309.
- Kennis, M., Rademaker, A.R., van Rooij, S.J., Kahn, R.S., Geuze, E., 2015b. Resting state functional connectivity of the anterior cingulate cortex in veterans with and without post-traumatic stress disorder. *Hum. Brain Mapp.* 36 (1), 99–109.
- Kessler, R.C., 2000. Posttraumatic stress disorder: the burden to the individual and to society. *J. Clin. Psychiatry* 61 (Suppl. 5), 4–12.
- Khanna, A., Pascual-Leone, A., Michel, C.M., Farzan, F., 2015. Microstates in resting-state EEG: current status and future directions. *Neurosci. Biobehav. Rev.* 49, 105–113. <http://dx.doi.org/10.1016/j.neubiorev.2014.12.010>. (Feb).
- Kikuchi, M., Koenig, T., Munesue, T., Hanaoka, A., Strik, W., Dierks, T., Koshino, Y., Minabe, Y., 2011. EEG microstate analysis in drug-naïve patients with panic disorder. *PLoS One* 6, e22912.
- Kindler, J., Hubl, D., Strik, W.K., Dierks, T., Koenig, T., 2011. Resting-state EEG in schizophrenia: Auditory verbal hallucinations are related to shortening of specific microstates. *Clin. Neurophysiol.* 122, 1179–1182.
- Koch, S.B., van Zuiden, M., Nawijn, L., Frijling, J.L., Veltman, D.J., Olf, M., 2016. Aberrant resting-state brain activity in posttraumatic stress disorder: a meta-analysis and systematic review. *Depress. Anxiety* 33 (7), 592–605.
- Koenig, T., Prichep, L., Lehmann, D., Sosa, P.V., Braeker, E., Kleinlogel, H., Isenhardt, R., John, E.R., 2002. Millisecond by millisecond, year by year: Normative EEG microstates and developmental stages. *NeuroImage* 16, 41–48.
- Lanius, R.A., Bluhm, R.L., Coupland, N.J., Hegadoren, K.M., Rowe, B., Theberge, J., Neufeld, R.W., Williamson, P.C., Brimson, M., 2010. Default mode network connectivity as a predictor of post-traumatic stress disorder symptom severity in acutely traumatized subjects. *Acta Psychiatr. Scand.* 121, 33–40.
- Lehmann, D., Ozaki, H., Pal, I., 1987. EEG alpha map series: Brain micro-states by space-oriented adaptive segmentation. *Electroencephalogr. Clin. Neurophysiol.* 67, 271–288.
- Liberzon, I., Sripada, C.S., 2007. The functional neuroanatomy of PTSD: a critical review. *Prog. Brain Res.* 167, 151–169.
- Lou, H.C., Luber, B., Crupain, M., Keenan, J.P., Nowak, M., Kjaer, T.W., Sackeim, H.A., Lisanby, S.H., 2004. Parietal cortex and representation of the mental self. *Proc. Natl. Acad. Sci. U. S. A.* 101 (17), 6827–6832.
- Lui, S., Huang, X., Chen, L., Tang, H., Zhang, T., Li, X., Li, D., Kuang, W., Chan, R.C., Mechelli, A., Sweeney, J.A., Gong, Q., 2009. High-field MRI reveals an acute impact on brain function in survivors of the magnitude 8.0 earthquake in China. *Proc. Natl. Acad. Sci. U. S. A.* 106, 15412–15417.
- Mandelkow, H., Halder, P., Boesiger, P., Brandeis, D., 2006. Synchronization facilitates removal of MRI artefacts from concurrent EEG recordings and increases usable bandwidth. *NeuroImage* 32, 1120–1126.
- Mantini, D., Perrucci, M.G., Del Gratta, C., Romani, G.L., Corbetta, M., 2007. Electrophysiological signatures of resting state networks in the human brain. *Proc. Natl. Acad. Sci.* 104, 13170–13175.
- Menon, V., Uddin, L.Q., 2010. Saliency, switching, attention and control: a network model of insula function. *Brain Struct. Funct.* 214, 655–667.
- Miller, D.R., Hayes, S.M., Hayes, J.P., Spielberg, J.M., Lafleche, G., Verfaellie, M., 2017. Default mode network subsystems are differentially disrupted in posttraumatic stress disorder. *Biol. Psychiatry* 2 (4), 363–371.
- Misaki, M., Phillips, R., Zotev, V., Wong, C.K., Wurfel, B.E., Krueger, F., Feldner, M., Bodurka, J., 2017. Connectome-wide investigation of altered resting-state functional connectivity in war veterans with and without posttraumatic stress disorder. *NeuroImage Clin.* 17, 285–296.
- Montgomery, S.A., Asberg, M., 1979. A new depression scale designed to be sensitive to change. *Br. J. Psychiatry* 134, 382–389.
- Musso, F., Brinkmeyer, J., Mobascher, A., Warbrick, T., Winterer, G., 2010. Spontaneous brain activity and EEG microstates. A novel EEG/fMRI analysis approach to explore resting-state networks. *NeuroImage* 52 (4), 1149–1161.
- Nishida, K., Morishima, Y., Yoshimura, M., Isotani, T., Iriwasa, S., Jann, K., Dierks, T., Strik, W., Kinoshita, T., Koenig, T., 2013. EEG microstates associated with salience and frontoparietal networks in frontotemporal dementia, schizophrenia and Alzheimer's disease. *Clin. Neurophysiol.* 124 (6), 1106–1114 (Jun).
- Pitman, R.K., Rasmusson, A.M., Koenen, K.C., Shin, L.M., Gilbertson, M.W., Milad, M.R., Liberzon, I., 2012. Biological studies of post-traumatic stress disorder. *Nat. Rev. Neurosci.* 13 (11), 769–787.
- Rabinak, C.A., Angstadt, M., Welsh, R.C., Kenndy, A.E., Lyubkin, M., Martis, B., Phan, K.L., 2011. Altered amygdala resting-state functional connectivity in post-traumatic stress disorder. *Front. Psych.* 14 (2), 62.
- Rauch, S.L., Shin, L.M., Phelps, E.A., 2006. Neurocircuitry models of posttraumatic stress disorder and extinction: human neuroimaging research—past, present, and future. *Biol. Psychiatry* 60 (4), 376–382.
- Seeley, W.W., Menon, V., Schatzberg, A.F., Keller, J., Glover, G.H., Kenna, H., Reiss, A.L., Greicius, M.D., 2007. Dissociable intrinsic connectivity networks for salience processing and executive control. *J. Neurosci.* 27 (9), 2349–2356.
- Sheline, Y.I., Price, J.L., Yan, Z., Mintun, M.A., 2010. Resting-state functional MRI in depression unmasks increased connectivity between networks via the dorsal nexus. *Proc. Natl. Acad. Sci. U. S. A.* 107, 11020–11025.
- Smith, S.M., Fox, P.T., Miller, K.L., Glahn, D.C., Fox, P.M., Mackay, C.E., Filippini, N., Watkins, K.E., Toro, R., Laird, A.R., Beckmann, C.F., 2009. Correspondence of the brain's functional architecture during activation and rest. *Proc. Natl. Acad. Sci. U. S. A.* 106 (31), 13040–13045. <http://dx.doi.org/10.1073/pnas.0905267106>.
- Shin, L.M., Liberzon, I., 2010. The neurocircuitry of fear, stress, and anxiety disorders. *Neuropsychopharmacology* 35, 169–191.
- Shin, L.M., Lasko, N.B., Macklin, M.L., Karpf, R.D., Milad, M.R., Orr, S.P., Goetz, J.M., Fischman, A.J., Rauch, S.L., Pitman, R.K., 2009. Resting metabolic activity in the cingulate cortex and vulnerability to posttraumatic stress disorder. *Arch. Gen. Psychiatry* 66, 1099–1107.
- Shirer, W.R., Ryali, S., Rykhlevskaia, E., Menon, V., Greicius, M.D., 2012. Decoding subject-driven cognitive states with whole-brain connectivity patterns. *Cereb. Cortex* 22, 158–165.
- Snaith, R.P., Hamilton, M., Morley, S., Humayan, A., Hargreaves, D., Trigwell, P., 1995. A scale for the assessment of hedonic tone: the Snaith-Hamilton Pleasure Scale. *Br. J. Psychiatry* 167, 99–103.
- Sridharan, D., Levitin, D.J., Menon, V., 2008. A critical role for the right fronto-insular cortex in switching between central-executive and default-mode networks. *Proc. Natl. Acad. Sci. U. S. A.* 105, 12569–12574.
- Sripada, R.K., King, A.P., Welsh, R.C., Garfinkel, S.N., Wang, X., Sripada, C.S., Liberzon, I., 2012a. Neural dysregulation in posttraumatic stress disorder: evidence for disrupted equilibrium between salience and default mode brain networks. *Psychosom. Med.* 74 (9), 904–911.
- Sripada, R.K., King, A.P., Garfinkel, S.N., Wang, X., Sripada, C.S., Welsh, R.C., Liberzon, I., 2012b. Altered resting-state amygdala functional connectivity in men with post-traumatic stress disorder. *J. Psychiatry Neurosci.* 37 (4), 241–249.
- Talairach, J., Tournoux, P., 1988. Co-planar Stereotaxic Atlas of the Human Brain. 3-Dimensional Proportional System: An Approach to Cerebral Imaging.
- Veer, I.M., Beckmann, C.F., van Tol, M.J., Ferrarini, L., Milles, J., Veltman, D.J., Aleman, A., van Buchem, M.A., van der Wee, N.J., Rombouts, S.A., 2010. Whole brain resting-

- state analysis reveals decreased functional connectivity in major depression. *Front. Syst. Neurosci.* 4 (pii: 41).
- Weathers, F.W., Huska, J., Keane, T.M., 1991. The PTSD Checklist Military Version (PCL-M). National Center for PTSD, Boston, MA.
- Weathers, F., Keane, T., Davidson, J., 2001. Clinician-administered PTSD Scale: a review of the first ten years. *Depress. Anxiety* 13, 132–156.
- Whalley, M.G., Kroes, M.C.W., Huntley, Z., Rugg, M.D., Davis, S.W., Brewin, C.R., 2013. An fMRI investigation of posttraumatic flashbacks. *Brain Cogn.* 81 (1), 151–159.
- Wong, C.K., Zotev, V., Misaki, M., Phillips, R., Luo, Q., Bodurka, J., 2016. Automatic EEG-assisted retrospective motion correction for fMRI (aE-REMCOR). *NeuroImage* 129, 133–147.
- Yan, X., Brown, A.D., Lazar, M., Cressman, V.L., Henn-Haase, C., Neylan, T.C., Shalev, A., Wolkowitz, O.M., Hamilton, S.P., Yehuda, R., Sodickson, D.K., Weiner, M.W., Marmar, C.R., 2013. Spontaneous brain activity in combat related PTSD. *Neurosci. Lett.* 547, 1–5.
- Yuan, H., Perdoni, C., Yang, L., He, B., 2011. Differential electrophysiological coupling for positive and negative BOLD responses during unilateral hand movements. *J. Neurosci.* 31, 9585–9593.
- Yuan, H., Zotev, V., Phillips, R., Drevets, W.C., Bodurka, J., 2012. Spatiotemporal dynamics of the brain at rest — exploring EEG microstates as electrophysiological signatures of BOLD resting state networks. *NeuroImage* 60, 2062–2072.
- Yuan, H., Zotev, V., Phillips, R., Bodurka, J., 2013. Correlated slow fluctuations in respiration, EEG, and BOLD fMRI. *NeuroImage* 1 (79), 81–93.
- Yuan, H., Young, K.D., Phillips, R., Zotev, V., Misaki, M., Bodurka, J., 2014. Resting-state functional connectivity modulation and sustained changes after real-time functional magnetic resonance imaging neurofeedback training in depression. *Brain Connect.* 4 (9), 690–701.
- Yuan, H., Ding, L., Zhu, M., Zotev, V., Phillips, R., Bodurka, J., 2016. Reconstructing large-scale brain resting-state networks from high-resolution EEG: spatial and temporal comparisons with fMRI. *Brain Connect.* 6 (2), 122–135.
- Zotev, V., Yuan, H., Phillips, R., Bodurka, J., 2012. EEG-assisted retrospective motion correction for fMRI: E-REMCOR. *Neuroimage* 63 (2), 698–712. <http://dx.doi.org/10.1016/j.neuroimage.2012.07.031>. (Nov 1).
- Zotev, V., Phillips, R., Yuan, H., Misaki, M., Bodurka, J., 2014. Self-regulation of human brain activity using simultaneous real-time fMRI and EEG neurofeedback. *NeuroImage* 85 (3), 985–995.